

# Morphology of a Breached Embankment Due to Overtopping Flow

Zainab Mohamed Yusof<sup>1\*</sup>, Ahmad Khairi Abd. Wahab<sup>2</sup>, Zulhilmi Ismail<sup>2</sup>,  
Shahabuddin Amerudin<sup>3</sup>

<sup>1</sup>Eco-hydrology Centre, Faculty of Engineering,  
Universiti Teknologi Malaysia, 81310 Johor Bahru, Johor, MALAYSIA

<sup>2</sup>Centre for Coastal and Ocean Engineering, Faculty of Engineering,  
Universiti Teknologi Malaysia, 81310 Johor Bahru, Johor, MALAYSIA

<sup>3</sup>Faculty of Built Environment and Surveying,  
Universiti Teknologi Malaysia, 81310 Johor Bahru, Johor, MALAYSIA

\*Corresponding Author

DOI: <https://doi.org/10.30880/ijie.2021.13.01.026>

Received 31 May 2020; Accepted 13 December 2020; Available online 25 February 2021

**Abstract:** An embankment is a man-made hydraulic structure, is built to provide flood control. It also presents risks to property and life due to their potential to fail and causes catastrophic flooding. In order to mitigate these risks, authorities and regulators need to carefully analyse and inspect embankment dams to identify potential failure modes and protect against them. This paper presents embankment failure morphology and the amount of erosion due to overtopping flow. The breached morphology is analysed for an embankment slope of 1V:3H. The embankment is constructed in the laboratory using a medium sand grain size of non-cohesive soil. The dimension of embankment height is 0.1 m and has been tested with inflows rate of  $Q = 0.8 \times 10^{-3} \text{ m}^3/\text{s}$ . Experimental results showed that the breached peak discharge is influenced by the morphology of the sediment eroded. The volume loss calculation of the embankment erosion is calculated using SURFER 8, indicating the volume of  $0.01 \text{ m}^3$  with the peak breached discharge of  $3.63 \times 10^{-3} \text{ m}^3/\text{s}$ , respectively. In comparison with FLOW-3D software, the volume loss predicted was  $0.0173 \text{ m}^3$ , which was approximately 43% difference higher than the experimental result.

**Keywords:** Embankment erosion, breached hydrograph, embankment volume loss and overtopping flow

## 1. Introduction

Embankment failures are presented by the sudden release of fluid or water contained in the reservoir behind the vertical barrier. There are two primary tasks and strategies in the analysis to determine the consequences of the potential embankment failure, which are the prediction of the outflow hydrograph, and the routing of that hydrograph through the downstream valley [1]. Prediction of the outflow hydrograph is significant, particularly when it poses a risk to the population located near the dam. For examples, mudflows and flash flood may occur, as a result of an embankment failure. Damage to property is assured and there is a risk of loss of life in the areas impacted by floods. Overtopping flow over an embankment may cause the breach. It is one of the significant causes happens worldwide due to inadequate spillway capacity, foundation defects, and piping and seepage [1], [2]. The concentration of sediment after the failure at downstream affects the flow of the river, which causes floods. The affected near-downstream population will have an impact on the effects of dam failures such as floodplains [14]. Therefore, morphology pattern of sediment transported

downstream due to embankment failure is crucial to analyse the consequences of risks and to minimise the impact of water washout on people and the environment.

The failure of the embankment dam is influenced by several factors such as overtopping flow, improper design of foundation and construction [4]. There are two leading causes of the breach problems, i.e. due to overtopping and piping failure [10]. The overtopping is the cause of the majority of dam failures [1], [11], [13]. In analysing the embankment failure, there are two parameters involved, which are (a) determination of the peak flow and (b) morphology of the failure modes. The reason for the embankment dam to failure is due to overtopping, which means it erodes the crest of the embankment and later develops to a breach through the embankment. The process of dam failure accelerates the sediment entrainment into the flow and causes significant embankment erosion. In many cases of embankment failure, the bottom of the breach will continually erode downwards until it reaches the bottom of the dam. Thus, suspended load gradually transported downstream concerning time and caused sand deposition until the embankment reaches a maximum failure.

Many studies have been carried out to understand the failure mechanism of an embankment due to overtopping. Understanding the various failure mechanisms that contribute to the breach process is essential in accurately assessing the risk of failure. This is because natural processes such as soil erosion, sediment transport morphology are highly complex. Therefore, numerical modelling was developed since the 1950s to understand the breaching process. Even though the process is challenging, but it is crucial for hydro scientists and engineers to understanding the process [7]. Sediment transports, for example, play essential roles in various geological phenomena. Thus, it is important to find out the characteristics of the sediment during the process of the embankment failure, particularly for a non-cohesive soil. In the present study, the aim is to understand the breach process in the laboratory works in order to determine the volume lost after the breached. The results are then compared with FLOW-3D model for validation.

## 2. Embankment Breaching

Embankment material or sediments in natural water are classified into two types, which are cohesive soil such as clay and silt; and non-cohesive types such as sand, gravel, coarse silt and cobble. Both types of particle have their properties. Cohesive sediment will undergo sediment transport mainly in floc; floc is formed due to large electrostatic forces. However, for non-cohesive sediment, the process of sediment transport will occur in disperse formation [6]. Therefore, in analysing sediment transport, a few parameters need to be established, such as Shields' particle mobility, grain size, bed slope, water depth, flow velocity, and sediment concentration. The first three parameters deal with bedload transport, while the other two is dealt with total sediment transport.

In theory, there are three hydraulic flow regimes and erosion zones for flow overtopping an embankment [5]. A highly erodible zone occurs when the subcritical flow happens on the dam crest. At this stage, the energy slopes, velocities, and tractive stresses are relatively low and cause the embankment crest to erode. The study found that the supercritical flow occurs at the downstream zone of the dam crest. At this region, the energy slope, tractive stress are much higher compare to a subcritical flow regime, and the erosion may observe at this phase. The third erosion zone in the downstream of the dam, the flow will accelerate at supercritical depth until reach uniform flow condition, changes of the surface slope may initiate erosion of sediment transport for non-cohesive embankment due to high tractive stress.

Chinnarasri [15] have investigated the erosion of homogeneous embankment due to overtopping to determine the flow pattern by experimenting. From the experiment, he stated that after the overtopping has occurred, the damage could be classified into four stages, as illustrated in Fig. 1. Zone 1 is the region where less erosion might happen due to subcritical flow approaching the embankment, and the flow velocities and shear stresses above the crest are relatively low. Further along the crest, a so-called transition zone from subcritical to critical flow is observed (illustrated as Zone 2). This zone exhibited high stresses due to the changes in the energy slope. Zone 3 is an area with a high potential for erosion. The flow started to accelerate rapidly along the downstream slope, resulting in increased shear stresses at the downstream corner of the crest. In the process, the velocities over the embankment downstream face accelerate, causing the sediment entrainment into the flow and cause significant embankment erosion. In many cases of dam failure, the bottom of the breach will continually erode downwards until it reaches the bottom of the dam. Thus, suspended load gradually transported downstream concerning time and caused sand erosion until the embankment reaches a maximum failure. The formation of sediment typically changes along the length of the channel due to continuous flowing water [12]. There is a variety of shape to represent breach morphology, including rectangular, triangular, trapezoidal, parabolic, and semi-circular, among others. At the moment, there does not appear to be a method by which an exact breach shape can be computed.

Meanwhile, a breach hydrograph resulting from embankment failures are unique in their time characteristic, in comparison to floods due to heavy rainfalls. For instance, inflow floods into dam reservoirs due to surface runoff. The breach hydrograph generally experiences a similar process, where the breach discharge increases until it reaches the peak outflow. The outflow discharge then will decrease and stop when the breach process ends. The hydrograph due to dam breach will have a much higher peak flow,  $Q_p$ , and shorter time to peak,  $t_p$ . There will be a delay that is known as lag time or breach initiation time,  $t_L$  that is representing the time interval between the initiation of the runoff or outflow. The rising limb of the breach outflow hydrograph is characterised by non-linear increase and followed by gradually increasing due to the sudden release of a large volume of water [13].

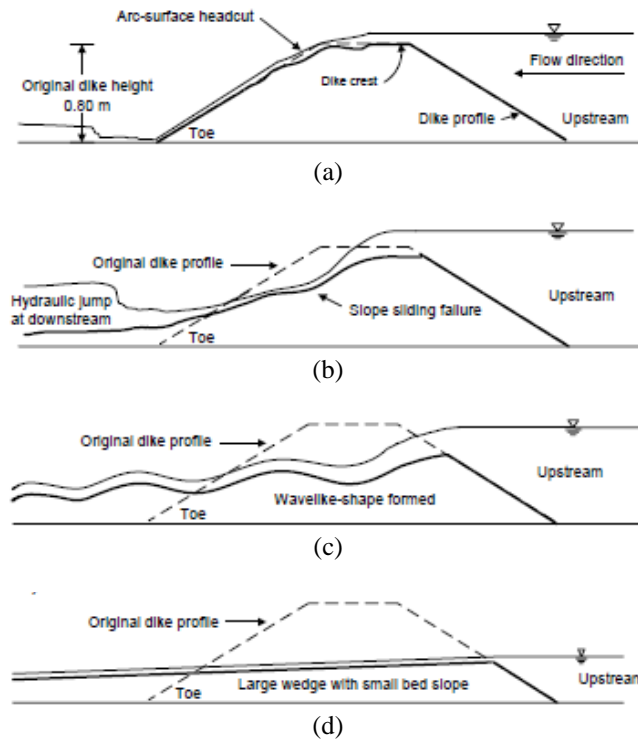


**Fig. 1 - Process of dike erosion due to overtopping: (a) Initial stage with small erosion on dike crest; (b) The second stage with slope sliding failure; (c) The third stage with wave shape formed; (d) The last stage with large wedge formed [15]**

### 3. Experimental Apparatus and Procedures

The breaching test for the embankment was carried out and took place at the Hydraulics and Hydrology Laboratory, Department of Hydraulics and Hydrology, Faculty of Civil Engineering. The testing was conducted in a 11 m long x 0.6 m deep x 0.5 m wide flume, as shown in Fig. 2. The water is pumped from the water tank to flowing from upstream to the downstream channel by passing through the embankment dam located at the middle of the channel, as illustrated in Fig. 3. Two cameras were installed to capture the progression of temporal embankment breaching to view from the top and front side. Then a v-notch is built at the end of the channel to measure the breached hydrograph during the breaching process. As for the embankment material, non-cohesive soil is used to construct the 0.1 m high embankment. The width of the embankment crest is 0.1 m. The face slope of the embankment is compacted and fixed at 1V:3H, as shown in Fig. 4. The breaching test uses a constant inflow rate of  $0.8 \times 10^{-3} \text{ m}^3/\text{s}$ . The inflow keeps constant until the overtopping process started and the water enters through the notch above the embankment crest.



**Fig. 2 - Experimental setup: (a) A 11 m long x 0.6 m deep x 0.5 m wide flume; (b) a V-notch to measure discharge**

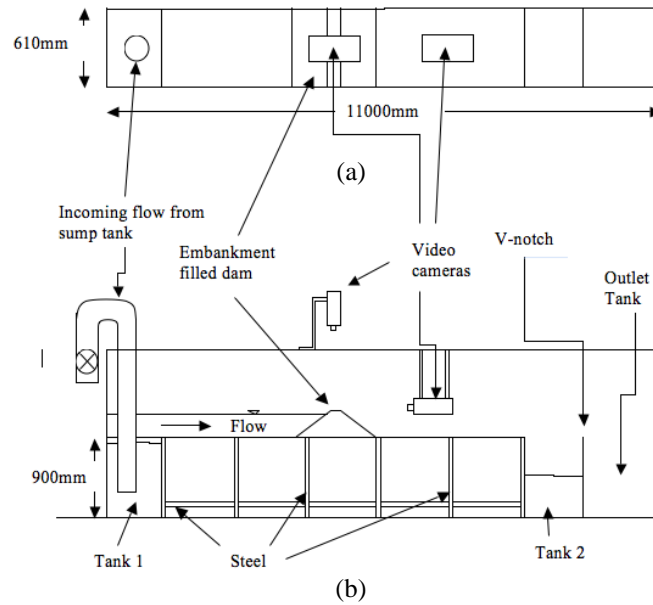


Fig. 3 - A schematic diagram of a channel setup: (a) plan view; (b) side view

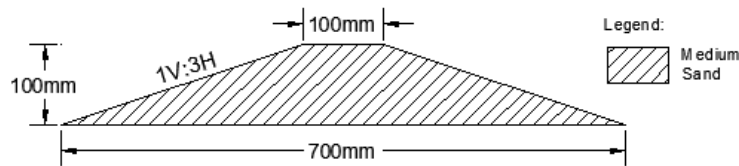


Fig. 3 - An embankment size used in the laboratory

The present study uses a physical model of 1:100, referring to a study conducted by Orendoff [12]. In the study, he stated a dam breaching is dominated by gravity forces and Froude scaling due to its complex interaction between sediment and fluid flow. Therefore, proper scaling of the embankment is possible using Froude scaling. The details of the scaling model constructed, shown in Table 1.

Table 1 - The prototype versus physical model properties of embankment

Prototype	Model
Length $L_p/L_m$	1:100
Channel length, $L_p = 1,100$ m	Channel length, $L_m = 11$ m
Channel width, $L_p = 60$ m	Channel width, $L_m = 0.6$ m
Embankment height, $L_p = 10$ m	Embankment height, $L_m = 0.1$ m
Sediment size Smaller than 2 mm	Medium Sand = 0.6 mm – 0.2 mm

As for the embankment compaction procedures, the initial testing procedure was sieving the material of non-cohesive soil, which is in a range between 600 $\mu$ m and 250 $\mu$ m. Material sieved was compacted layers by layers to form the embankment at the middle of the channel, as shown in Fig. 5(a). The embankment compaction took place in two lifts of 50 mm each with water was sprayed for the ease of the compaction works. At the centre of the embankment crest, a notch was built, as shown in Fig. 5(b). It functioned as the weak point of the embankment dam. The notch size was 10 mm in height and 30 mm in width.



**Fig. 5 - Compacting the embankment: (a) compaction method; (b) a notch as the weak point of the embankment**

Once the initial breach is formed, the hydrodynamic force continues to enlarge it by eroding the soil material. The eroded sediment was transported by water downstream. It must be emphasized that little is known about the mechanic of non-homogeneous sediment transport, especially under highly dynamic conditions, such as existing for dam breach. Thus, one has to resort to employing sediment transport method based on the experience from alluvial streams. During the experiment, video cameras were used to record the temporal progression of breaching patterns. The discharge is then measured using a V-notch with a 90° angle, located at the outlet of the flume. The discharge is calculated using the formulae of flow over a weir, as in Eq. (1).

$$Q = \frac{8}{15} \times C_d \times \sqrt{2g} \times \tan\left(\frac{\theta}{2}\right) H^{\frac{5}{2}} \quad (1)$$

where  $Q$  is the rate of discharge ( $m^3/s$ ),  $C_d$  is the coefficient of discharge, which takes a value of 0.61,  $g$  is the acceleration due to gravity,  $\theta$  is the angle of the V-notch and  $H$  is the height of water flowing through the notch. Eq. (1) is then used to obtain the hydrograph by plotting the discharge value against the time taken during the test. The value of peak outflow and time to peak is determined from the hydrograph obtained. Meanwhile, the water depth at the V-notch is measured using a point gauge to calculate the outflow discharge, as illustrated in Fig. 2(b).

#### 4. SURFER 8 Analysis

The analysis of volume calculation is carried out using a SURFER 8 program. It uses to contour a 3D surface mapping of embankment breached using shading and colours to emphasise the elevation data. The volume value of the surfaces created for specific reference surface,  $z = 0$  is calculated according to the rules of Trapezoidal rule, Simpson's rule and Simpson's 3/8 rule. The difference between these calculation rules depends on the different interpolation methods and grid ranges. Fig. 6 shows the grid used to record the data for the 3D surface modelling.

After the embankment has completely breached, the sediment morphology is recorded using a point gauge to determine the height of the sediment at a grid. Then the data is plotted in 3 axes;  $x_n$ ,  $y_n$ , and  $z_n$  ( $n = 1, 2, 3, \dots$ ) whereby  $y_n$  is sediment height at each point of the grid intersection of  $x$  and  $y$  axes. Each grid is fixed to 5 cm for  $x$ -axis and  $z$ -axis, while, the  $y$ -axis represents the height of the sediment recorded.

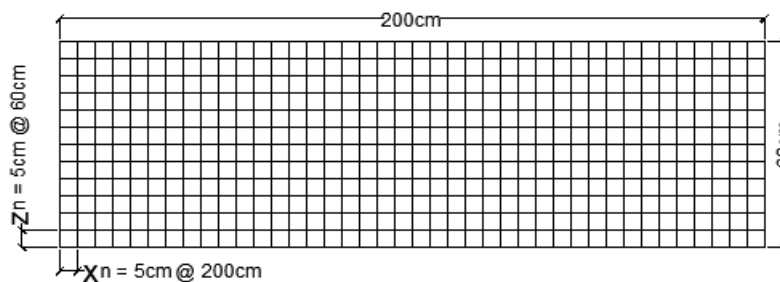


**Fig. 6 - A plan view of grids created as an intersection point to measure the sediment heights**

### 5. Results and Discussion

The breaching process starts when the flow enters into the notch as the result of overtopping flow. This is due to the fact that the water forces the embankment material been eroded. Also, the effect of hydrostatic forces behind the embankment triggers the embankment material to be transported away due to instability to cause failure to the embankment. After the breaching process has been completed, half of the embankment has been eroded by the stream and formed such bed locks, as shown in Fig. 7(b). The formation of sediment eroded to the downstream is varies based on the input of flow rates and compaction degree of the sediment.



**Fig. 7 - Experimental morphology of an embankment failure: (a) Initial breaching; (b) after completely breached**

When the embankment starts to breach, it continues to erode parts of the embankment. The process was initiated from the weakness part of the sediment. In this study, the final shape of the breached embankment due to erosion was almost symmetrical between both sides, which has a similar result found in [9]. Fig. 8 shows a plot of breached morphology and breached hydrographs after the embankment has completely breached. The heights of sediment remaining were recorded and plotted in SURFER 8 software for the volume loss calculation. The data was recorded for 5 seconds interval. The result of the peak flow rate for breach outflow hydrograph obtained was approximately  $3.63 \times 10^{-3} \text{ m}^3/\text{s}$ , which is occurred at 105 s, as shown in Fig. 9. Once the flow enters the notch (at  $t = 0 \text{ s}$ ), the overtopping begins and causes the breaching, approximately after 70 s. The erosion starts at the middle of the embankment (the notch) and widens laterally before eroding vertically like a trapezoidal shape from a front view. This might due to the initial shape of v-notch built at the crest of the embankment to trigger the erosion. When the water starts to flow through the notch, erosion takes place slowly at the middle of the crest until the embankment fails. The severe failure is due to hydrostatic pressures exerted on it, and this can be observed from the sharp changes in the hydrograph produced. The volume of the failure embankment is then measured and calculated using SURFER 8. The volume before the failure is approximately  $0.024 \text{ m}^3$ , which is close to the exact value of the theoretical calculation. After the failure, the remaining embankment volume calculated was approximately  $0.014 \text{ m}^3$  for all the calculation methods (rules) from the SURFER software. The results indicate that the volume loss of the failure embankment due to erosion was approximately  $0.0079 \text{ m}^3$ , as indicated in Table 2. Fig. 8 illustrates the erosion pattern of the breached embankment from the SURFER 8 analysis.

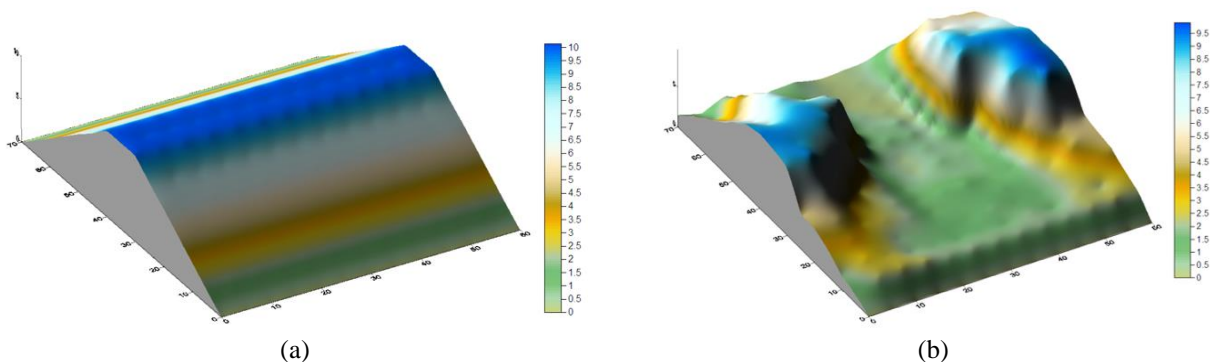


**Fig. 8 - 3D surface morphology using SURFER 8 of an embankment failure: (a) Before and (b) After failure. The legend (in colours) represents the elevation in cm**

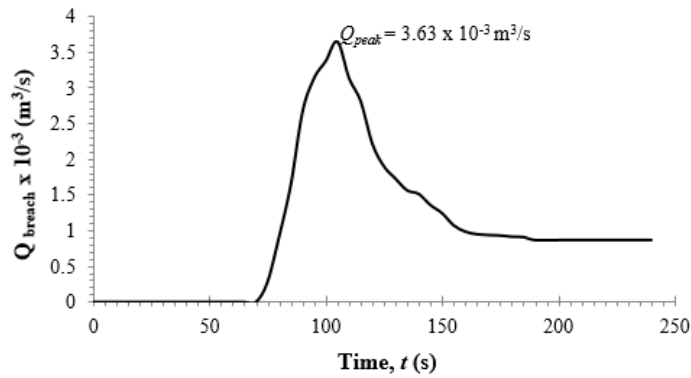


Fig. 9 - A breached hydrograph of the embankment failure

### 6. FLOW-3D Validation

The simulation results using the FLOW-3D version 11 are presented as a validation. The model setup is similar to the set up in the laboratory. The sediment scours model in FLOW-3D uses a packed sediment as bedload transport to simulate the erosion. A packed bed is an erodible solid object that is used to represent solid objects in the hydrodynamic solver. The morphological change in the packed bed is governed by the conservation of sediment mass. The model used the Meyer-Peter and Muller with a critical Shields number of 0.05, entrainment coefficient 0.018, and a bed load coefficient of 8; as default values in the model setup. The embankment is made of two sediment grain sizes: 0.3 mm and 0.4 mm, and a density of 2080 kgm<sup>-3</sup>. This material is closely similar to the experimental of breach embankment where the grain size ranging from 0.2 mm – 0.5 mm. Fig 10 shows the initial and boundary conditions of the model setup in FLOW-3D.

Results on free surface elevation for a specific time, are shown in Fig. 11. As the flow enters the notch, the flow accelerates onto the embankment downstream face, so-called overland sheet flow. At this point, the embankment erodes at the surface and tends to deepen the erosion vertically, as shown in Fig. 11(a), and laterally in Fig. 11(b) to Fig.11(d). **Error! Reference source not found.** 12 plots the breached hydrograph and remaining embankment volume after the breach is completed. It showed that after approximately 250 s of the simulation time, there is no breaching occurred. The result indicated that the peak flow occurred at  $t = 78$  s, with a maximum peak discharge of  $5.19 \times 10^{-3} \text{ m}^3\text{s}^{-1}$ . Meanwhile, the remaining embankment volume at a peak time was  $0.012 \text{ m}^3$ . The embankment continually eroded until the flow became stable after approximately 200 s. The final remaining embankment volume recorded was  $0.007 \text{ m}^3$ .

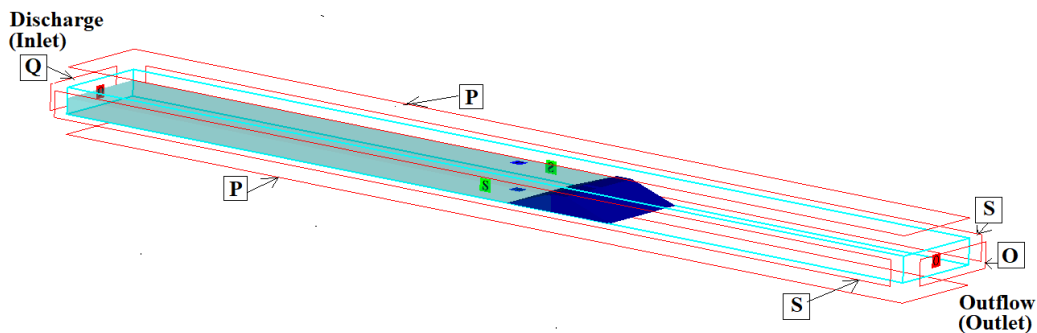
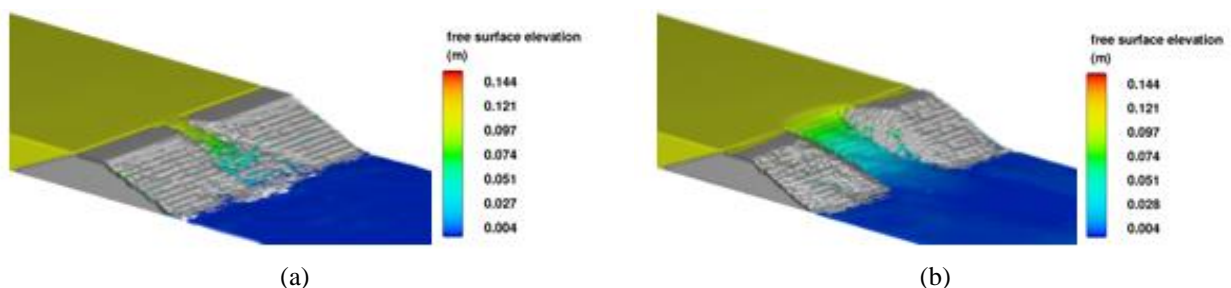
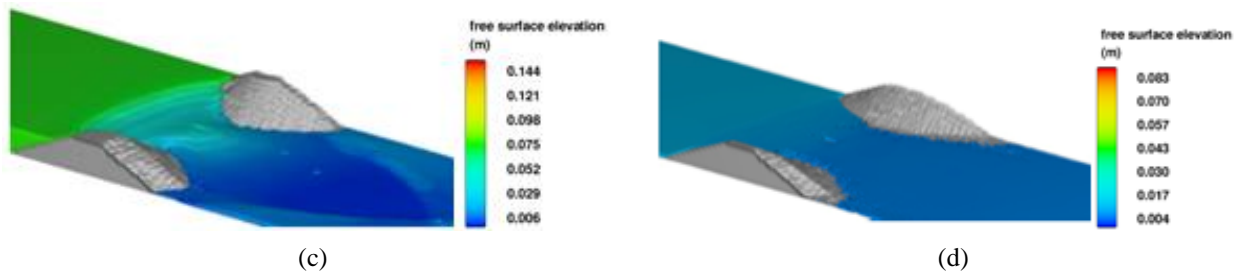
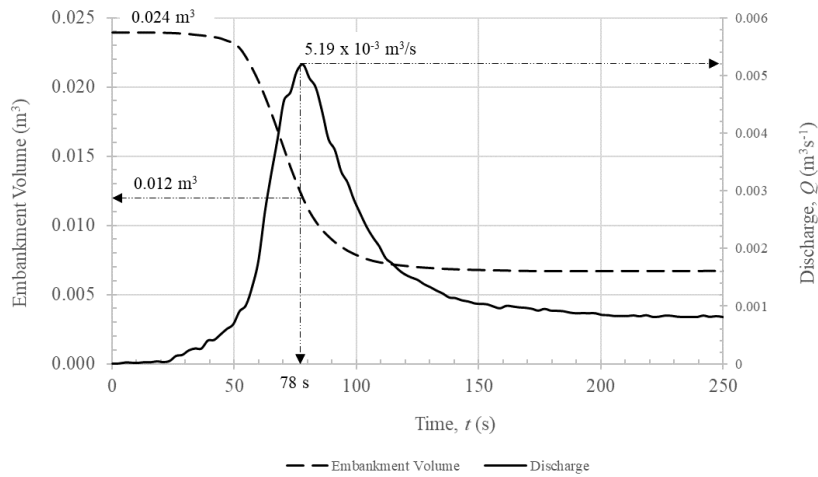


Fig. 10 - Initial and boundary conditions setup: S– symmetry, Q – Discharge (inlet), O – Outflow (outlet) and P- Specified Pressure. The dark blue represents the embankment, and the light blue area represents the initial flow depth





**Fig. 11 - Temporal progression of free surface flow over the breached area: (a)  $t = 40$  s; (b)  $t = 60$  s; (c)  $t = 78$  s; and (d)  $t = 250$  s**



**Fig. 12 - The breach hydrograph and embankment volume during the breaching time**

Table 2 shows the comparison results of volume loss and the breached hydrograph between FLOW-3D and the experimental results of Case Study E1. The volume loss calculation from the experiment using the Trapezoidal Rule in SURFER and MATLAB analysis was found the same value of approximately  $0.01 \text{ m}^3$ . However, in FLOW-3D, the embankment volume loss calculated was  $0.017 \text{ m}^3$ , which gave a percentage difference of 42.7%. As for the breach of hydrograph analysis, FLOW-3D predicted difference of 30.2%. Similarly, the result of time to reach the peak flow indicates a difference of 34.6%. The analysis showed that the FLOW-3D predicts more erosion compared to the experimental results. This might due to the characteristics of the packed sediment arrangement setup in FLOW-3D, which affects the numerical method's results in the transport equation.

**Table 2 – Comparison results of Volume Loss between FLOW-3D and SURFER 8**

Volume Calculation Method	Volume Before Failure ( $\text{m}^3$ )	Volume After Failure ( $\text{m}^3$ )	Volume Lost ( $\text{m}^3$ )	Peak Discharge ( $\text{m}^3\text{s}^{-1}$ ) $\times 10^{-3}$	Peak time (s)
Trapezoidal Rule (SURFER)	0.02396	0.014	0.0099	3.63	51
FLOW-3D	0.02394	0.007	0.0173	5.20	78
% Difference			42.7	30.2	34.6

## 7. Conclusion

The present study is to understand the formation of sediment erosion due to embankment failure to the breached hydrograph, the morphology of sediment eroded and the amount of embankment volume loss. Failures at the middle of the embankment showed the sediment is being eroded more even as compared to the upper downstream face surface. The width of the sediment erosion also became narrower as compared to the upstream that transported more extensive towards the wall of the channel. As a result, sediment erosion towards the breach area tends to form a tapered shape leading to a trapezoidal breached. The results also showed a relationship between the amounts of volume loss to the hydrograph produced. The analysis has shown that the flow rate of  $0.8 \times 10^{-3} \text{ m}^3/\text{s}$  would give a volume loss of the breached embankment for about 43%.difference between experimental and model. The finding concludes that the characteristics of the embankment failures influence the embankment morphology patterns. In summary, it can be said the higher flow

rate through the initially breached embankment will result in more sediment to be transported to downstream. The rapid the erosion, the more volume of the embankment will be eroded.

## Acknowledgement

The authors would like to express sincere thanks to University Teknologi Malaysia and Ministry of Higher Education Malaysia for funding this research with GUP grant, Tier 1 (UTM/ Q.J130000.2522.09H07) and School of Civil Engineering for providing facility and equipment during the research.

## References

- [1] Wahl, T. L. (2010). Dam Breach Modelling – An Overview of Analysis Hydraulic. Engineer Bureau of Reclamation Denver, Colorado
- [2] Wahl, T. L. (1998). Prediction of Embankment Dam Breach Parameters: A Literature Review and Needs Assessment Dam Safety. Research Report DSO-98-004, U.S. Department of the Interior Bureau of Reclamation Denver, Colorado
- [3] Pugh, C. A. (1985). Hydraulic Model Studies of Fuse Plug Embankments. Research Report REC-ERC-85-7, U.S. Department of the Interior Bureau of Reclamation Denver, pp 33
- [4] Singh, V. P. (1996). Dam Breach Modeling Technology. Massachusetts: Kluwer Academic Publisher
- [5] Powledge, G. R., Ralston, D. C., Miller, P., Chen, Y. H., Clopper, P. E. & Temple, D. M. (1989). Mechanics of overflow erosion on embankments II: Hydraulic and design considerations. *Journal of Hydraulic Engineering*, 20, 1056-1075
- [6] Wu, W. (2011). Earthen embankment breaching. *Journal of Hydraulic Engineering*, 137(12), 1549-1564
- [7] Yusof, Z., Hargreaves, D. & Morvan, H. (2010). Development of a porous model to characterise erosion of a breached embankment. 1<sup>st</sup> European Congress of the IAHR, Edinburgh
- [8] Wang, Z. & Bowles, D. S. (2006). Three-dimensional non-cohesive earthen dam breach model part 1: Theory and methodology. *Advances in Water Resources*, 29(10), 1528-1545
- [9] Lazin, M. N. A. (2014). Erodible Dam Breaching Patterns due to Overtopping. Master Thesis, Universiti Teknologi Malaysia
- [10] Pickert, G., Weitbrecht, V. & Bieberstein, A. (2011). Breaching of overtopped river embankments controlled by apparent cohesion. *Journal of Hydraulic Research*, 49(2), 143-156
- [11] Schmocker, L. & Hager, W. (2009). Sediment Transport Models to Simulate Erosion of Overtopped Earth-Dikes. Zurich: Laboratory of Hydraulic Hydrology and Glaciology, pp 499-507
- [12] Orendorff, B. (2009). The Effect of Initial Breach Geometry on Dam Breach Morphology. PhD Thesis, University of Ottawa
- [13] Al-Riffai, M. (2010). Breach channel morphology in the unsaturated zone and under various compaction densities. CDA 2010 Annual Conference Niagara Falls. Canada: Canadian Dam Association
- [14] Mohamed Yusof, Z., Omar, N. A. & Amerudin, S. (2015). Floodplain modelling due to dam break. *Jurnal Teknologi*, 75(10), 135-142
- [15] Chinnarasri, C. (2003). Flow pattern and damage of dike overtopping. *International Journal of Sediment Research*, 10, 301-309